

Presulfidation and activation mechanism of Mo/Al₂O₃ catalyst sulfided by ammonium thiosulfate

Mingxing Tang, Hui Ge, Weibin Fan, Guofu Wang, Zhanjun Lyu, and Xuekuan Li[†]

State Key laboratory of Coal Conversion Institute of Coal Chemistry, Chinese Academy of Sciences, Taiyuan 030001, China
(Received 12 October 2013 • accepted 10 February 2014)

Abstract—Mo/Al₂O₃ catalyst was presulfided with (NH₄)₂S₂O₃ to elucidate presulfidation and activation mechanism. It is illustrated that the Mo oxide is firstly partially sulfided during presulfidation and then in situ reduced into MoS_{2-x} in activation, and finally sulfided to active state during hydrodesulfurization (HDS). A synergistic effect between the S²⁻ and S⁶⁺ ions in (NH₄)₂S₂O₃ produces a positive influence on the HDS performance. The S²⁻ ions contribute to the sulfidation of Mo ions, while the S⁶⁺ species interact with Al₂O₃ support, weakening the interaction of active species with support.

Keywords: Hydrodesulfurization, Ammonium Thiosulfate, Presulfidation, Activation, Support Interaction

INTRODUCTION

Mo-based hydrodesulfurization (HDS) catalysts have been used in industrial hydrotreating processes for decades [1]. Commercial HDS catalysts are usually available in an oxide form and must be activated by a gas or liquid sulfiding agent, such as H₂S, CS₂ or CH₃SSCH₃ (DMDS) [2-4]. However, the use of such malodorous and noxious compounds causes environmental pollution and is harmful to the operators. Presulfidation technologies, due to their environmentally friendly character and easy operation, have attracted much interest by refineries [5-7], where the oxide catalysts are presulfided in advance with a solution of elemental sulfur or polysulfide followed by heat-treatment, to partially convert the metal oxide to sulfides. Then, the partly sulfided catalyst is loaded into reactor for hydrogen activation. The catalytic activity of sulfided catalyst is strongly influenced by the nature of the sulfiding agent and the activation conditions [8,9].

The in situ sulfidation of HDS catalysts by gas or liquid sulfiding agents has been extensively studied [10-16]. Unpromoted Mo/Al₂O₃ is often used as model catalyst to reveal the relations between active phase and HDS performance. With ESR, XPS and Raman spectroscopies, different intermediates such as oxysulfides and MoS₃ can be identified in various proportions during temperature-programmed sulfidation. But in final catalyst, the Mo is mainly present as MoS₂; however, the morphology and structure of MoS₂ may be considerably different, depending on the state of the oxide precursor, the sulfiding agent, and the temperature and duration of sulfidation [17].

In alumina-supported (Co)Mo sulfide at least two type of phases were observed: single-layer type I phase is only partially sulfided owing to the strong Mo-O-Al linkages with the support; multi-layer type II phase can be fully sulfided due to a weak interaction with alumina [18], the type II phase shows an activity twice as that of the type I phase [19]. Dugulan et al. [20] found that (Co)Mo/Al₂O₃

sulfided at high-pressure shows much higher HDS activity than at 1 atm due to formation of Type II Co-Mo-S phase. DFT calculation reveals that the formation of Mo-O-Al linkages increases the energy to remove sulfur atoms from the active surface to form coordinatively unsaturated Mo sites (CUS), which is considered the active site of HDS [21]. The Mo-O-Al linkages are preferred to locate at the S edge in MoS₂ slabs. Both Mo and S edges may form CUS but with different catalytic properties [23]; the nature of exposed edges depends on the preparation and activation conditions [24].

The sulfiding conditions impose important effects on the morphology, dispersion and structures of MoS₂ slabs, and consequently HDS activity. An insight into the sulfidation and activation mechanism is beneficial to the application of presulfidation process. However, few studies have contributed to such a process. In previous work we found that Mo-based catalyst presulfided with (NH₄)₂S₂O₃ showed high sulfidation degree and HDS activity [25]. In this paper, we focus on the presulfidation and activation mechanism of (NH₄)₂S₂O₃.

EXPERIMENTAL

1. Catalyst Preparation

The γ -Al₂O₃ support was impregnated with a concentrated ammonium solution of (NH₄)₆Mo₇O₂₄·4H₂O by the pore filling method. The impregnated sample was dried at 110 °C for 12 h and calcined at 450 °C for 4 h. The prepared Mo/Al₂O₃ catalyst contained 8 wt% Mo. The Mo/Al₂O₃ catalysts were presulfided by two methods: 1) Mo/Al₂O₃ catalysts calcined at 450 or 600 °C was impregnated with an aqueous solution of (NH₄)₂S₂O₃ by the pore filling method, and dried at 90 °C for 2 h. These obtained samples were denoted as MoS3-450 and MoS3-600, respectively. 2) The γ -Al₂O₃ support catalyst was co-impregnated with the ammonium solution of (NH₄)₆Mo₇O₂₄·4H₂O and (NH₄)₂S₂O₃, and dried at 90 °C for 2 h; the obtained catalyst is designated as MoS3-dry. The Mo content of MoS3-dry catalysts was also 8 wt% after calcinations. The presulfided catalysts have an S/Mo molar ratio of 3.0.

2. Activation and HDS Activity of the Prepared Catalysts

The activation and the HDS test were carried out in a fix-bed micro reactor. The catalyst loading was 0.1 g (40-60 mesh), without includ-

[†]To whom correspondence should be addressed.

E-mail: lxx@sxicc.ac.cn

Copyright by The Korean Institute of Chemical Engineers.

ing presulfiding agent and absorbed water. Presulfided catalyst was in situ activated under hydrogen. For presulfided catalyst, the system was heated from room temperature to 300 °C at a rate of 5 °C/min and a pressure of 3.0 MPa under a hydrogen flow of 33 mL/min. Then it was kept at 300 °C for 0.5 h, followed by cooling to the reaction temperature of 280 °C. For comparison, the Mo/Al₂O₃ catalyst was sulfided with a flow of DMDS solution (1.5 wt% DMDS in nonane, 0.08 mL/min) at 3.0 MPa flowing hydrogen (33 mL/min). The detailed procedures are as follows: The reactor was first heated to 200 °C, and then the sulfiding feed was introduced; the temperature was first kept for 2 h, followed by increasing from 200 to 350 °C at a rate of 2.5 °C/min; the sulfidation was then continued for 4 h; finally the reactor was cooled to reaction temperature.

The HDS of thiophene was performed at 280 °C in a H₂ flow (3.0 MPa, 33 mL/min). 1.5 wt% thiophene in nonane was pumped into the reactor at a liquid velocity of 0.08 mL/min. The product oil was collected in a liquid collector and measured on a Shimadzu GC-14B chromatograph packed with an OV-101 capillary column and equipped with an FID detector. The spent catalysts were washed with n-hexane solvent and sealed under Ar into glass bottle for characterizations.

3. Catalyst Characterization

High resolution transmission electron microscopic (HRTEM) images of the spent catalysts were obtained on a JEOL JEM-2010 microscope operated at 200 kV. For estimation of the stacking and size distribution of MoS₂ crystallites, more than 400 crystallites were measured. The average slab length and stacking degree were calculated according to following equation: $\bar{M} = \frac{\sum_{i=1}^n n_i M_i}{\sum_{i=1}^n n_i}$, where M_i is the slab length or number of slabs of a MoS₂ unit and n_i the number of slabs or stacks in a determined range of length or stacking number.

For the fresh catalysts, the total sulfur content was measured by chemical analysis [26]. The S²⁻ content of the spent catalyst was performed on a micro coulometer (KZDL-3, Hebi-gaoke, China) by coulomb titration method. The carbon content in spent catalyst was measured by combustion method [27].

The surface area and pore properties of the catalysts were measured by nitrogen adsorption at 77 K with a Tristar 3000 (Micromeritics Instrument Co., USA). Before analysis, the catalysts were degassed at 60 °C for dried samples or at 200 °C for other samples in a vacuum of 0.13 Pa for 6-8 h.

Thermogravimetry-mass spectrometer (TG-MS) tests were conducted on a Setaram TGA92 thermogravimetry instrument connected with an OmniStar 200 quadrupole mass spectrometer. The connecting pipes were heated at 200 °C to avoid deposition of effluents. In each run, ca. 30 mg catalyst was loaded, and the temperature was ramped from room temperature to 600 °C at a rate of 10 °C/min. The m/z signals of H₂ (2), H₂O (18), S (32), H₂S (34), SO₂ (64) and SO₃ (80) in effluents were recorded by mass spectrometer. The experiments on presulfided catalysts were conducted under reductive atmosphere (10% H₂-90% Ar). For comparison, a sample of (NH₄)₂S₂O₃/Al₂O₃ was prepared by impregnation of alumina support with the same amount of ammonium thiosulfate used in presulfided catalysts. This sample was measured under reductive gas and simulating air (21% O₂-79% Ar).

X-ray photoelectron spectra (XPS) were measured on a Physi-

cal Electronics Company Quantum-2000 Scanning ESCA Microprobe spectroscope (Al Kα). Each sample was loaded in a glovebox and transported into the instrument under N₂ protection. Binding energy (BE) was calibrated with signal of contaminated carbon at 284.6 eV.

The temperature programmed desorption of ammonia (NH₃-TPD) was performed using a quartz micro reactor TP-5000 (Tianjing-Xianquan, China). About 50 mg sample was loaded in each run. The sample was first pretreated in an Ar flow of 50 mL/min at 500 °C for 2 h, and then cooled to 120 °C. This was followed by pulse-injecting enough ammonia. Further, the sample was flushed with the Ar flow at 120 °C for 1 h to remove physically adsorbed ammonia. Finally, the temperature was raised from 120 to 500 °C at a rate of 10 °C/min. The amount of desorbed NH₃ was measured with a thermal coupled detector (TCD). The profiles of NH₃-TPD were deconvolved by Gaussian method.

RESULTS

1. Thiophene HDS Activity

Fig. 1 shows the conversion of thiophene vs. time on stream. At least 8-10 hours was needed for MoS₃-dry and MoS₃-450 to achieve stability. During this period, the thiophene HDS activity increased with the time on stream. This suggests that the catalysts might not be well sulfided during hydrogen activation. They were continually sulfided by thiophene during HDS reaction. At initial stage, the MoS₃-450 showed higher thiophene conversion than MoS₃-dry. However, after about 5 h, the MoS₃-dry surpassed MoS₃-450. Owing to no calcinations applied to the MoS₃-dry, this catalyst was presented at wet status and was more difficult to be effectively sulfided. Contrarily, MoS₃-600 and Mo/Al₂O₃ seem to have been sufficiently sulfided during activation. No apparent stabilized duration was observed. MoS₃-600 was calcined at 600 °C before impregnation with ammonium thiosulfate. Although the high temperature calcination had negative effect on the HDS activity, the catalyst was easier to achieve stabilization. Because the Mo/Al₂O₃ was effectively sulfided by DMDS, the HDS activity maintained stable during the test.

It is clear that the HDS activities of presulfided catalysts were

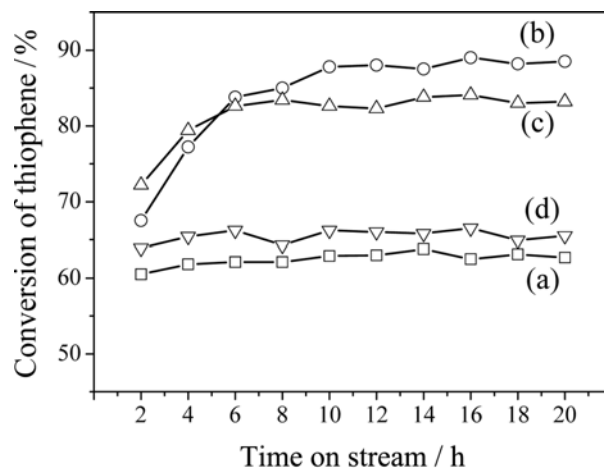


Fig. 1. Thiophene conversion vs. time on stream over (a) Mo/Al₂O₃, (b) MoS₃-dry, (c) MoS₃-450, (d) MoS₃-600. Reaction conditions: 3.0 MPa, V(H₂)/V(oil)=412, LHSV=4.0 h⁻¹.

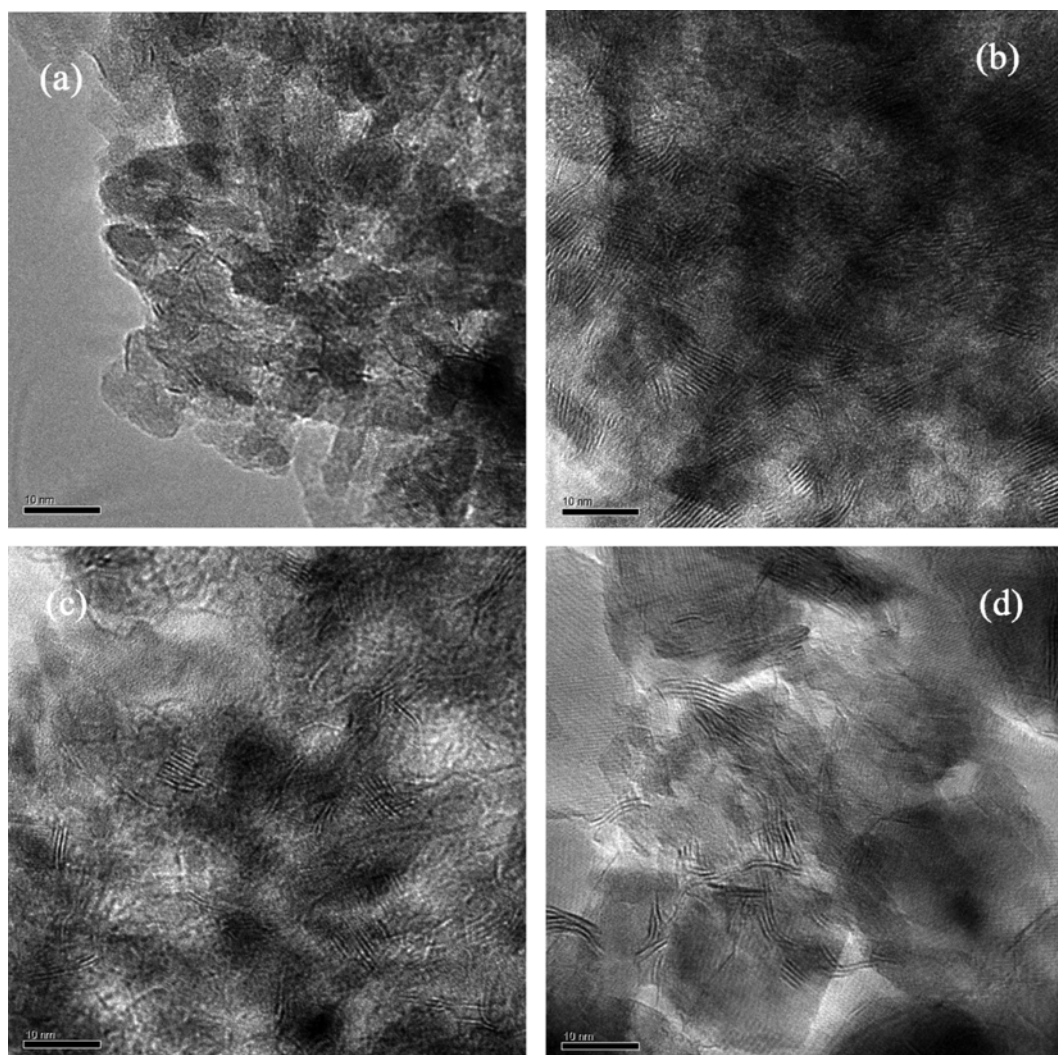


Fig. 2. HRTEM images of spent catalysts: (a) Mo/Al₂O₃, (b) MoS₃-dry, (c) MoS₃-450, (d) MoS₃-600.

higher than that of DMDS sulfided catalyst. Ammonium thiosulfate had positive influence on the thiophene conversion. For pre-sulfided catalysts, the calcinations conditions had important impact on the initial and final catalytic activity. If calcinations were applied to catalysts before impregnating with sulfiding agent, hydrogen activation was easier. The stabilization duration was at the sequence of MoS₃-600 < MoS₃-450 < MoS₃-dry. However, the final HDS activity was at the sequence of MoS₃-600 < MoS₃-450 < MoS₃-dry.

2. HRTEM Observation

The dispersion and morphology of the spent catalysts were investigated by HRTEM. The side-view images of MoS₂ hexagonal base

planes with 0.62 nm inter-plane distance are shown in Fig. 2. Mo/Al₂O₃ possesses single layer MoS₂ structures (Type I), while the pre-sulfided catalysts show mainly double or multi-layer MoS₂ slabs (Type II) [28]. The mean width and stacking number of MoS₂ slabs are calculated by measuring over 400 MoS₂ slabs. The results are listed in Table 1. The mean width and stacking number of Mo/Al₂O₃ are only 2.4 nm and 1.1, respectively, much smaller than those of pre-sulfided catalysts. The strong interaction between MoS₂ slabs with Al₂O₃ prevents the active crystallites to grow. The pre-sulfided catalysts show similar mean width of MoS₂ slabs. This illustrates that the different preparations have less influence on the mean width,

Table 1. Analysis of sulfur and carbon content in spent catalysts

Catalysts	C contents (wt%)	Molar ratio of S ²⁻ /Mo	MoS ₂ particles	
			Ave. width (nm)	Ave. stacking No.
Spent Mo/Al ₂ O ₃	0.2	1.7	2.4	1.1
Spent MoS ₃ -dry	3.3	1.9	3.2	3.4
Spent MoS ₃ -450	1.9	1.8	3.2	3.0
Spent MoS ₃ -600	1.5	1.3	3.2	2.5

but the stacking number increased with the decrease of the treatment temperature applied to the Mo metals. This suggests that the presulfidation technology can effectively decrease the interaction of active phase with support. High treatment temperature to Mo metal increased the interaction between active metal and support.

3. Sulfur and Carbon Element Analysis

Using the sulfur chemical analysis, the S/Mo molar ratios of fresh MoS₃-dry MoS₃-450 and MoS₃-600 are 2.9, 3.0 and 2.9, respectively. These are almost the same as those added, indicating no sulfur losses during the presulfiding process. The S²⁻/Mo mole ratios of spent catalysts are listed in Table 1. The spent MoS₃-dry and MoS₃-450 had S²⁻/Mo ratios of 1.9 and 1.8, respectively, close to the stoichiometric ratio of ideal MoS₂ crystal. This indicates a sufficient sulfidation. In contrast, the S²⁻/Mo molar ratio of the spent MoS₃-600 is only 1.3; this is due to high temperature calcinations leading to some of Mo ions into Al₂O₃ support and formation of Al₂(MoO₄)₃; this part of Mo is difficult to sulfide [29]. The DMDS sulfided Mo/Al₂O₃ has an S²⁻/Mo molar ratio of 1.6, lower than the stoichiometric ratio of MoS₂. This is a result of the strong interaction of Mo with Al₂O₃, which inhibits the sulfidation of Mo ions. The carbon content decreased in the order of MoS₃-dry > MoS₃-450 > MoS₃-600 > Mo/Al₂O₃. The presulfided catalysts contained higher amount of carbon than the parent catalyst. The carbon species might modify active phase or exist as coke [30].

4. BET Analysis

To investigate the influence of ammonium thiosulfate on the physical properties of catalyst, BET analysis was carried out on the fresh and the spent catalysts, as well as support (Table 2). For the fresh MoS₃-dry and MoS₃-450, the surface areas and pore volumes decreased apparently after being impregnated with Mo metal and ammonium thiosulfate, although the pore diameter was not apparently changed. The decreased degree of surface area and pore volume is much larger for the MoS₃-600, accompanied with the increase in the average pore size. This is due to collapse of pores at high calcination temperature. After HDS reaction, the surface area of Mo/Al₂O₃ was not changed, but pore volume and average pore size dropped slightly. In contrast, the surface areas of MoS₃-dry and MoS₃-450 had recovered to the level of the parent catalyst, while the pore volume and the average pore diameter were slightly smaller than that of Mo/Al₂O₃. This indicates that the presulfidation did not change the support porosity. The decrease in the pore volume and the average pore size may be due to the block of pores by carbon species. Never-

Table 2. Textural properties of fresh and spent catalysts

Catalysts	Average pore diameter (nm)	Pore volume (cm ³ /g cat)	BET surface area (m ² /g cat)
γ-Al ₂ O ₃	8.0	0.46	230
Fresh Mo/Al ₂ O ₃	9.1	0.40	176
Fresh MoS ₃ -dry	8.1	0.24	120
Fresh MoS ₃ -450	9.8	0.24	116
Fresh MoS ₃ -600	26.2	0.14	21
Spent Mo/Al ₂ O ₃	8.3	0.37	178
Spent MoS ₃ -dry	7.5	0.32	170
Spent MoS ₃ -450	8.2	0.33	164
Spent MoS ₃ -600	16.9	0.24	56

theless, the surface area and the pore volume of MoS₃-600 were much less than those of Mo/Al₂O₃. The average pore size is almost twice as much as that of Mo/Al₂O₃. This evidenced the collapse of the support.

5. TG-MS Test

Fig. 3 shows the TG-DTG profiles over different samples. Three weight loss regions were observed below 250 °C for (NH₄)₂S₂O₃/Al₂O₃ (Fig. 3(a)). SO₂ and a small amount of SO₃ was detected by MS between 150 and 350 °C. The ammonium thiosulfate is an unstable compound, which decomposes at about 150 °C in air to ammonium sulfurous acid, sulfur, ammonium and water, etc. The weight loss below 100 °C is ascribed to the desorption of absorbed water, while loss in the range of 100-250 °C is attributed to the decomposition of ammonium thiosulfate.

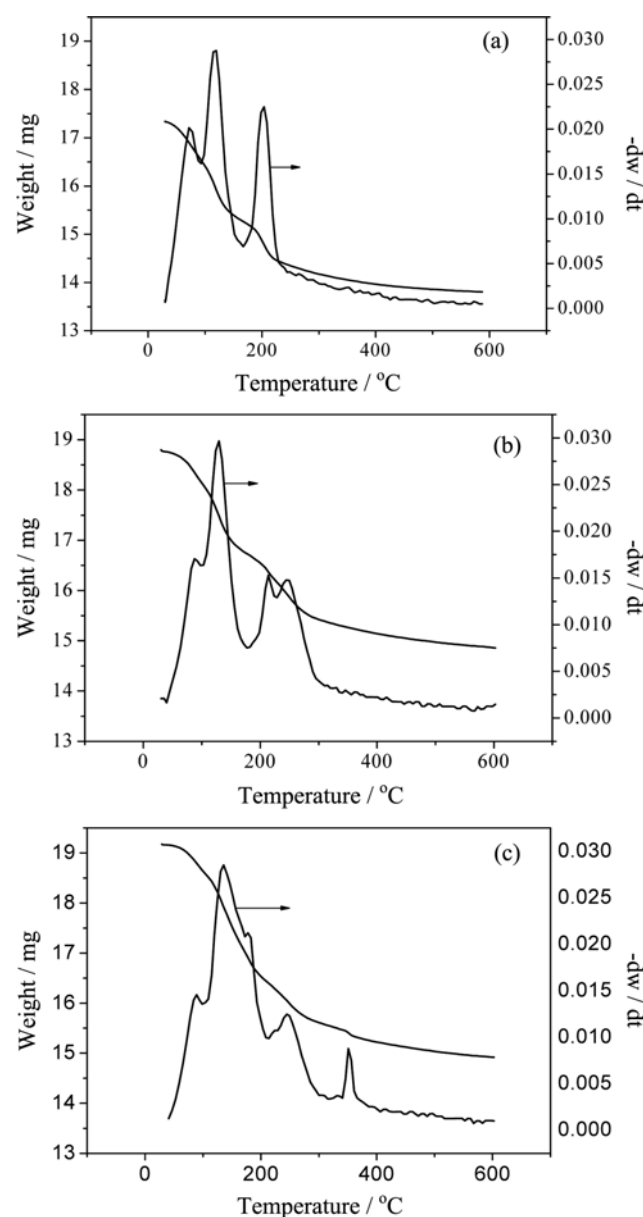


Fig. 3. TG-DTG spectra of samples: (a) (NH₄)₂S₂O₃/Al₂O₃ in 20% O₂-80% Ar; (b) (NH₄)₂S₂O₃/Al₂O₃ in 10% H₂-90% Ar; (c) MoS₃-dry in 10% H₂-90% Ar.

Table 3. XPS analysis of catalysts after H₂ activation and after HDS reaction

Catalyst	Mo3d _{5/2} (eV)	Fraction (%)	S 2p _{3/2} (eV)	Fraction (%)	S ⁶⁺ /S ²⁻	S ²⁻ /Mo
MoS3-dry after activation	227.9 (1.6)	75	161.4 (1.4)	81	0.2	0.7
	229.3 (1.3)	12	167.2 (3.0)	19		
	231.8 (2.1)	13				
MoS3-450 after activation	228.5 (2.3)	61	161.7 (2.5)	75	0.3	0.9
	231.0 (1.2)	8	169.0 (2.1)	25		
	232.6 (2.3)	31				
MoS3-600 after activation	228.5 (1.9)	55	161.6 (2.7)	77	0.2	0.9
	230.9 (1.3)	20	169.0 (2.4)	23		
	232.6 (1.1)	25				
MoS3-dry after HDS	228.4 (1.5)	74	161.5 (1.9)	76	0.1	1.7
	230.5 (2.9)	9	168.5 (2.1)	23		
	232.2 (1.9)	17				
MoS3-450 after HDS	228.5 (1.7)	71	161.4 (1.8)	84	0.2	1.7
	230.7 (2.0)	15	168.2 (2.1)	16		
	232.2 (1.6)	14				
MoS3-600 after HDS	228.6 (1.9)	63	161.2 (1.7)	81	0.2	1.3
	230.0 (2.5)	13	168.7 (1.7)	19		
	231.9 (2.1)	24				
Mo/Al ₂ O ₃ after HDS	228.4 (1.9)	71	161.2 (1.6)	100	0.0	1.6
	230.0 (1.5)	15				
	231.7 (2.0)	14				

*The full widths at half maximum are given in parentheses

Four weight loss regions were observed for (NH₄)₂S₂O₃/Al₂O₃ heated in reductive atmosphere (Fig. 3(b)). The first three regions are similar to those observed in air atmosphere. Between 200 and 250 °C, SO₂ and H₂S was observed by MS. This suggests that the fourth weight loss region might be attributed to reductive decomposition of residues formed through the decomposition of (NH₄)₂S₂O₃ at lower temperature.

The different (NH₄)₂S₂O₃ presulfided catalysts showed similar TG-DTG profiles; thus as an example the TG/DTG curves of MoS3-dry in reductive gas atmosphere were shown. Clearly, there are five weight loss regions. The regions corresponding to DTG peaks at 90 and 135 °C are due to desorption of water and initial decomposition of (NH₄)₂S₂O₃, while ones around 180 and 250 °C can be attributed to the reductive decomposition of (NH₄)₂S₂O₃. For the weight loss larger than 300 °C, MS measurement shows that a large amount of hydrogen was consumed although no sulfur species can be detected around this temperature. According to ref. [31], during sulfidation of Mo-based catalysts, the Mo⁶⁺ ions are reduced to Mo⁴⁺ through the Mo⁵⁺ intermediates. The highest reduction rate was observed between 300 to 400 °C. Therefore, the weight loss larger than 300 °C could be ascribed to the reduction of Mo. From above results, we can conclude that the sulfidation of Mo mainly takes place between 130 and 300 °C, and reduction mainly occurs between 300 and 400 °C.

6. XPS Characterization

To investigate the change in valence and coordination of Mo and S ions during hydrogen activation and thiophene HDS reaction, XPS measurements were conducted over the catalysts after activation and HDS reaction, respectively. The Mo 3d_{5/2} with BE around 232 eV represents the oxidized Mo⁶⁺ species, the Mo 3d_{5/2} of sulfided

Mo⁴⁺ appears at about 228 eV, and Mo 3d_{5/2} at 230 eV is attributed to the Mo⁵⁺ intermediate ions of oxysulfide [32]. For the S 2p spectra, the BEs at about 162 and 168 eV is attributed to S²⁻ ligands and S⁶⁺ species, respectively [33]. The envelopes of Mo and S ions were deconvoluted by XPSPEAK 4.1 software and the relative content was calculated by the sensitive factors provided by instrument provider.

The XPS results are listed in Table 3. The S²⁻/Mo molar ratios of presulfided catalysts after activation and HDS reaction show large differences. The relative content of Mo⁶⁺, Mo⁵⁺ and Mo⁴⁺ is almost the same before and after HDS reaction for MoS3-dry, but its S²⁻/Mo ratio increases from 0.7 to 1.7. During activation the S²⁻ ligands may be stripped by hydrogen from the active surface [34]. This would result in a low S²⁻ content on the surface of the activated catalyst. However, the stripped sulfur can be supplemented by the sulfur of thiophene during HDS reaction. This also held true for MoS3-450 and MoS3-600, although the relative content of Mo⁴⁺ slightly increased during HDS reaction. This shows that besides the sulfur supplement, the reductive sulfidation of Mo also occurs during HDS reaction for these two presulfided catalysts. The results illustrate that the sulfidation for a presulfided catalyst can be well achieved through both ammonium thiosulfate presulfidation and HDS reaction.

Although the atomic ratio of S⁶⁺ to S²⁻ in ammonium thiosulfate is 1, the relative content of S⁶⁺ is much smaller than that of S²⁻ after activation. This discrepancy suggests that much more of S⁶⁺ ions are released in the form of SO₂, as shown by TG-MS. The remained sulfate species may primarily come from the Al₂(SO₄)₃·5H₂O, which can be detected in fresh presulfided catalyst by XRD [25].

7. NH₃-TPD Acidity Measurement

Fig. 4 shows the NH₃-TPD profiles of spent catalysts. The acid sites have been classified on the basis of an arbitrary range: weak

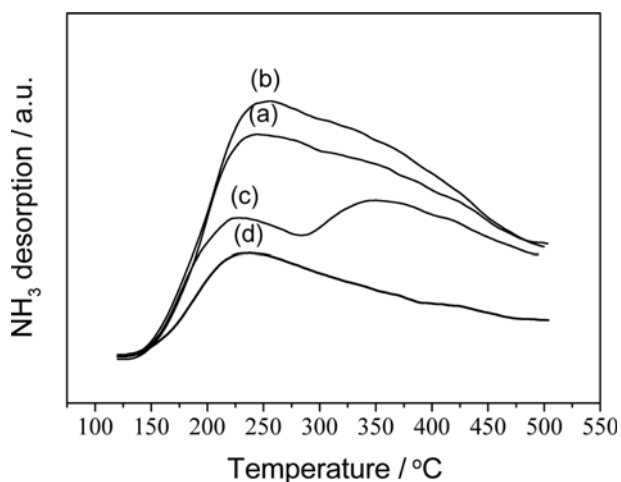


Fig. 4. NH₃-TPD curves of spent catalysts: (a) Mo/Al₂O₃, (b) MoS₃-dry, (c) MoS₃-450, (d) MoS₃-600.

(120–220 °C), medium (220–350 °C), and strong (350–550 °C) [35]. Table 4 compiles the number of weak, medium and strong sites obtained by such classification. As seen in this table, MoS₃-450 shows two types (weak and strong) of acid sites, while others possess the weak, medium and strong acid sites. Considering the total number of acid sites, the observed trend is: MoS₃-dry > Mo/Al₂O₃ > MoS₃-450 > MoS₃-600. Although the sulfate groups are present on the presulfided catalysts, the acidity does not increase. This suggests that the combination of sulfate groups with aluminum ions inhibited the formation of new acidic centers.

The acidities of the presulfided catalysts are significantly different. Because MoS₂ shows almost no acidity, the acidity of samples mainly comes from the acidic hydroxyl group of alumina support. The low acidity of MoS₃-600 is due to the condensation of hydroxyl groups of support caused by calcination at high temperature. In the Mo/Al₂O₃ catalyst, MoS₂ interacts strongly with basic hydroxyl groups of Al₂O₃ support [36], and thus the acidic sites on the support surface are kept almost intact. In contrast, for the presulfided catalysts, the sulfate species may compete with MoS₂ to interact with basic hydroxyl group. This would cause part of MoS₂ to interact with mediate acidic hydroxyl group, weakening the acidity of support. As a result, MoS₃-450 shows lower acidity than Mo/Al₂O₃. As for MoS₃-dry, no calcination was applied to the Mo precursor; thus, the surface hydroxyl groups were reserved, exhibiting slightly higher acidity.

DISCUSSION

In the presulfided catalyst, parts of the metal oxides are trans-

formed into oxysulfides or sulfides [37]. Moulijn et al. [11] reported that extensive O-S exchange occurs below 200 °C between MoO₃ and H₂S when H₂S is used to sulfide MoO₃/Al₂O₃. De Boer et al. [12] found through EXAFS that even at room temperature the O is also considerably exchanged with S in Mo/SiO₂.

In this experiment, the catalysts after impregnation with (NH₄)₂S₂O₃ were heat-treated at 90 °C for 2 h in air. The XRD results of our previous experiment evidenced the formation of Al₂(SO₄)₃·5H₂O phase [25,38]. It was proposed that a part of (NH₄)₂S₂O₃ is transformed into (NH₄)₂SO₄ through O-S exchange with Mo oxides, then the (NH₄)₂SO₄ intermediate reacts with Al₂O₃ to form Al₂(SO₄)₃·5H₂O. The XRD also showed that the other (NH₄)₂S₂O₃ were still reserved on the presulfided catalyst. During the hydrogen activation, this part of (NH₄)₂S₂O₃ decomposed and sulfided the Mo specie, and the Mo⁺⁶ ions were simultaneously reduced to Mo⁺⁴ ions. The TG-MS results show that the (NH₄)₂S₂O₃ decompose and produce H₂S and SO₂, etc., between 130 and 300 °C. The H₂S can react with Mo oxides or oxysulfides. The reductive reaction of Mo⁺⁶ occurs mainly at 300–400 °C. The XPS results shows that after activation the S²⁻/Mo molar ratio in the presulfided catalysts is much smaller than that (1.5) of fresh catalysts. This indicates that the S⁶⁺ ions in ammonium thiosulfate might not take part in the sulfidation of Mo ions.

By the temperature programmed sulfidation (TPS), Scheffer et al. [39,40] observed the H₂S release at about 225 °C. They proposed that the breaking of Mo-S bond of MoS₃ intermediate produces elemental sulfur, which is then reduced to H₂S. De Boer et al. [12] found in MoO₃/SiO₂ catalyst that increasing the temperature to 150 °C leads to the formation of MoS₃ analogies, which are transformed into MoS₂ between 250 and 300 °C. Payen et al. [14] could identify different proportions of intermediates, such as oxysulfide and MoS₃ during the sulfidation of MoO₃/Al₂O₃ by in situ Raman technology. However, de Jong et al. [41] could not find evidence for the formation of elemental sulfur when studying MoO₃/SiO₂/Si catalyst. They suggested that at low temperature MoO₂ or H_xMoO₃ species are included in the interior, while Mo⁺⁴ oxysulfides are formed on the surface.

In this study, the mole ratios of S⁶⁺/S²⁻ of presulfided catalysts were found to drop from 1.0 to 0.2–0.3 after hydrogen activation. The TG-MS experiment showed the SO₂ release under air or reductive atmosphere. Thus it is postulated that the initial decomposition of ammonium thiosulfate produced the elemental sulfur and SO₂. Then the elemental sulfur intermediate was reduced to H₂S, as shown in Eq. (1) and (2). And the (NH₄)₂SO₃ intermediate continually decomposed to release NH₃, H₂O and SO₂.



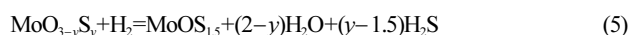
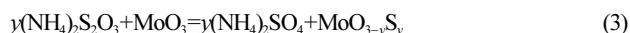
Table 4. Surface acidity of spent catalysts measured by TPD-NH₃

Catalysts	Total acidity (μmolNH ₃ /g)	Dispersion of acidity (μmolNH ₃ /g) (%)		
		Weak	Mediate	Strong
Spent Mo/Al ₂ O ₃	360	90 (25%)	137 (38%)	133 (37%)
Spent MoS ₃ -dry	417	163 (39%)	109 (26%)	144 (35%)
Spent MoS ₃ -450	230	76 (33%)	0	154 (67%)
Spent MoS ₃ -600	156	63 (40%)	80 (51%)	13 (9%)



By comparing the sulfiding intermediates in $MoO_3/SiO_2/Si(100)$ with the $(NH_4)_2[Mo_3S_{13}] \cdot H_2O$ cluster, Muijers et al. [42] thought that the sulfidation goes through a Mo^{5+} intermediate species ($MoOS_{1.5}$). Guichard et al. [43] found the Mo^{5+} oxysulfides in the sulfided Mo catalysts. The XPS results of the presulfided catalysts showed the existence of Mo^{5+} ions, suggesting the formation of Mo oxysulfides.

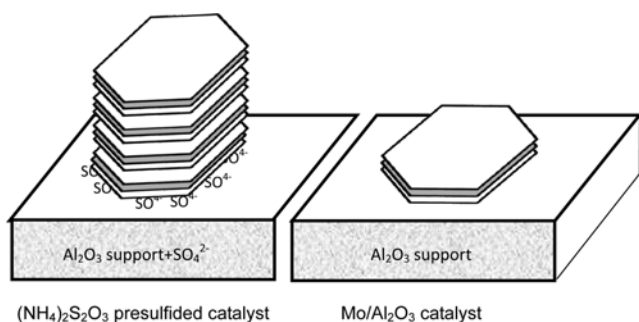
We deduced that (a) the Mo^{6+} oxysulfides intermediate are formed by O-S exchange during presulfidation and activation (as shown in Eqs. (3) and (4)), (b) the Mo^{5+} oxysulfides are formed in activation (Eq. (5)), (c) elemental sulfur intermediate originates from the decomposition of sulfiding agent, and (d) the MoS_2 intermediate may not form because of the limited supplication of H_2S in activation.



The HRTEM shows that the active phases of presulfided catalysts have multi-layer type II structures, and the DMDS sulfided Mo/Al_2O_3 shows mainly single MoS_2 slabs. Candia et al. [44] reported that in an increase in the sulfiding temperature from 400 to 600 °C, the structure of the active phase of $CoMo/Al_2O_3$ catalysts transformed from type I to type II. The type I active phase interacts strongly with alumina, forming Mo-O-Al linkage, whereas the type II structure exhibits only a weak van der Waals interaction with support. Catalysts with type II active phases show higher intrinsic activities [45]. The transformation of type I to type II can be made possible by addition of ligands, or use of support with weak interaction, such as carbon [46-51]. Prins et al. [52,53] found that passivation by air led to formation of sulfate species on sulfided $Co(Ni)Mo/Al_2O_3$ catalyst and induced the structure transformed from type I to type II $Co(Ni)-Mo-S$ active phase.

The XPS shows that the S^{6+} ions were present on the surface of the presulfided catalyst after activation and HDS reaction (Table 3). $Al_2(SO_4)_3 \cdot 5H_2O$ phase in the support should represent these sulfate species. It is deduced that the basic Al-OH group reacts with acidic sulfate species to form the $Al_2(SO_4)_3$. This resulted in the decrease of interaction of Mo with Al_2O_3 , and the formation of Type II MoS_2 structures, as illustrated in Scheme 1.

The effect of sulfate species on Mo/Al_2O_3 catalysts is comparable to that of phosphate. The phosphate has been extensively applied in refineries to improve HDS catalysts. After introduction of phos-

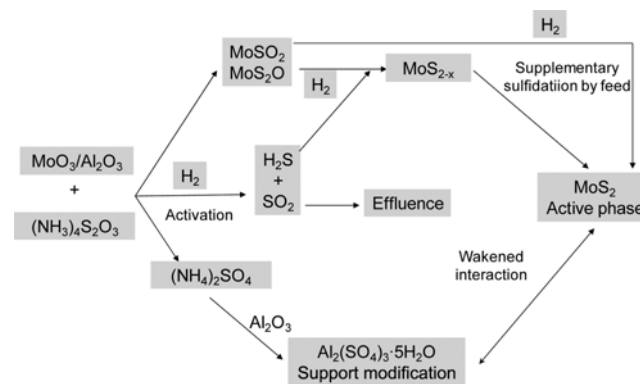


Scheme 1. Active phase and support models of $(NH_4)_2S_2O_3$ presulfided and DMDS sulfided Mo/Al_2O_3 catalysts.

phate, the $AlPO_4$ formed on the surface of alumina support decreases the interaction of support with oxide precursors [54]. HRTEM images showed that addition of phosphate increases the stacking number and width of MoS_2 crystallites in Mo/Al_2O_3 and $CoMo/Al_2O_3$ catalysts [55]. The enhancement in stacking suggests the formation of Type II Co-Mo-S structures. Our results show that the sulfate species in $(NH_4)_2S_2O_3$ presulfided catalysts plays a role similar to that phosphate does.

After hydrogen activation, the S^{2-}/Mo ratios of presulfided catalysts are smaller than 1.0 (Table 3). TG-MS measurement shows that the temperature for decomposition of $(NH_4)_2S_2O_3$ into SO_2 and H_2S is between 130 and 300 °C. However, only over 300 °C, sulfided Mo-based catalyst can catalyze the SO_2 gas reduced into elemental sulfur and H_2S under hydrogen atmosphere, the yield of H_2S increases with increasing temperature [56]. The SO_2 originating from decomposition of $(NH_4)_2S_2O_3$ cannot be reduced into H_2S in this experiment. Owing to the shortage of H_2S , the presulfided catalysts cannot be effectively sulfided during activation. However, after HDS reaction, the sulfiding degree has enhanced apparently. The S^{2-}/Mo of MoS3-dry and MoS3-450 have increased over 1.7. MoS3-600, owing to calcinations at the high temperature, shows less S^{2-}/Mo . We determined that during thiophene HDS a supplementary sulfidation occurs, namely, the sulfur removed from thiophene remains on the MoS_x active phases; thus the Mo is sulfided continually by thiophene. Meanwhile, some oxysulfide can be further sulfided to MoS_2 , as evidenced by XPS. The total sulfidation process is illustrated in Scheme 2. After the supplementary sulfidation, the $(NH_4)_2S_2O_3$ presulfided catalysts show much better HDS performance than Mo/Al_2O_3 sulfided by DMDS, as shown in Fig. 1.

From the above results and analyses, it could be concluded that during presulfidation and activation the S^{2-} ions in $(NH_4)_2S_2O_3$ sulfide the Mo ions, while S^{6+} species weaken the interaction of Mo with Al_2O_3 support and enhance the sulfiding degree. Their synergetic effect results in the formation of Type II MoS_2 active phases. On the other hand, the $(NH_4)_2S_2O_3$ presulfided catalysts showed similar or lower acidity compared to the catalyst sulfided by DMDS; this excludes the possibility that the HDS activity is facilitated by the crack of sulfur-containing compound. XPS results show that the MoS3-dry and MoS3-450 catalysts have a Mo^{4+} relative content similar to the DMDS sulfided catalyst, and MoS3-600 has lower Mo^{4+} relative content, excluding the enhancement in catalytic activ-



Scheme 2. Schematic presulfidation and activation mechanism of Mo/Al_2O_3 catalyst presulfided by $(NH_4)_2S_2O_3$.

ity by higher content of MoS₂. Although the high calcination temperature used for MoS₃-600 causes low sulfidation degree and Mo⁴⁺ relative content, this catalyst still showed higher HDS activity than DMDS sulfided Mo/Al₂O₃. This suggests that the formation of Type II MoS₂ is the main reason for the high catalytic activities of (NH₄)₂S₂O₃ presulfided catalysts and the sulfiding degree has less meaning for the HDS activity.

CONCLUSIONS

During impregnation of Mo/Al₂O₃ with (NH₄)₂S₂O₃, the Mo is partly sulfided through the O-S exchange; the intermediate of (NH₄)₂SO₄ reacts with Al₂O₃ support to form Al₂(SO₄)₃, which weakens the interaction of active metal with support. The Mo species are further sulfided by (NH₄)₂S₂O₃ and reduced by hydrogen in the activation process, and the multi-layer Type II MoS₂ active phases are formed. The insufficiency of S²⁻ ligands in presulfided catalysts resulted in a molar ratio of S²⁻/Mo lower than 1.0 after activation process. In HDS reaction, the S²⁻/Mo molar ratio was markedly enhanced through a supplementary sulfidation, being close to the ideal stoichiometric ratio of 2. The (NH₄)₂S₂O₃ presulfided catalysts show higher thiophene HDS activities than DMDS-sulfided Mo/Al₂O₃ catalyst. This is due to the formation of intrinsically highly active Type II phases in former catalyst. An increase in the sulfiding degree may also have a positive effect on the HDS activity. The different sulfur atoms in (NH₄)₂S₂O₃ play different roles; the S²⁻ sulfides the Mo ion, while the S⁶⁺ modifies the support. The cooperation of these two types of S ions makes the (NH₄)₂S₂O₃ presulfided catalysts exhibit excellent HDS activities.

ACKNOWLEDGEMENTS

We gratefully acknowledge the financial supports from National Basic Research Program of China (973) (2006CB202504).

REFERENCES

1. C. Song, *Catal. Today*, **86**, 211 (2003).
2. N. Frizi, P. Blanchard, E. Payen, P. Baranek, M. Rebeilleau, C. Dupuy and J. P. Dath, *Catal. Today*, **130**, 272 (2008).
3. K. L. Kim and K. S. Choi, *Korean J. Chem. Eng.*, **5**, 177 (1988).
4. S. Z. Abghari, S. Shokri, B. Baloochi, M. A. Marvast, S. Ghanizadeh and A. Behrooz, *Korean J. Chem. Eng.*, **28**, 93 (2011).
5. J. G. Welch, P. Poyer and R. F. Skelly, *Oil Gas J.*, **92**, 56 (1994).
6. P. Dufresne, N. Brahma and S. R. Muff, US Patent, 5,985,787 (1993).
7. M. de Wind, J. J. L. Heinerman, S. L. Lee and F. L. Plantenga, *Oil Gas J.*, **90**, 49 (1992).
8. W. Qian, S. Yamada, A. Ishihara, M. Ichinoseki and T. Kabe, *Sekiyu Gakkaishi*, **44**, 225 (2001).
9. H. Ge, X. Li, Z. Qin, F. Liang and J. Wang, *Korean J. Chem. Eng.*, **26**, 576 (2009).
10. F. E. Massoth, *J. Catal.*, **36**, 164 (1975).
11. P. Arnold, J. A. M. van den Heijkant, G. D. de Bok and J. A. Moulijn, *J. Catal.*, **92**, 35 (1985).
12. M. de Boer, A. J. van Dillen, D. C. Koningsberger and J. W. Geus, *J. Appl. Phys.*, **32**, 460 (1993).
13. T. H. Weber, J. C. Muijsers, J. H. M. C. van Wolput, C. P. J. Verhagen and J. W. Niemantsverdriet, *J. Phys. Chem.*, **100**, 14144 (1996).
14. E. Payen, S. Kasztelan, S. Houssenbay, R. Szymanski and J. Grimblot, *J. Phys. Chem.*, **93**, 6501 (1989).
15. R. Prada Silvy, P. Grange and B. Delmon, *Stud. Surf. Sci. Catal.*, **53**, 233 (1989).
16. A. M. de Jong, H. J. Borg, L. J. van Ijzendoorn, V. G. F. M. Soudant, V. H. J. de Beer, J. A. R. van Veen and J. W. Niemantsverdriet, *J. Phys. Chem.*, **97**, 6477 (1993).
17. J. Ramirez and F. Sanchez-Minero, *Catal. Today*, **130**, 267 (2008).
18. E. J. M. Hensen, V. H. J. de Beer, J. A. R. van Veen and R. A. van Santen, *Catal. Lett.*, **84**, 59 (2002).
19. Y. Okamoto, A. Kato, Usman, N. Rinaldi, T. Fujikawa, H. Koshika, I. Hiromitsu and T. Kubota, *J. Catal.*, **265**, 216 (2009).
20. A. I. Dugulan, E. J. M. Hensen and J. A. R. van Veen, *Catal. Today*, **130**, 126 (2008).
21. B. Hinnemann, J. K. Nørskov and H. Topsøe, *J. Phys. Chem. B*, **109**, 2245 (2005).
22. L. S. Byskov, J. K. Nørskov, B. S. Clausen and H. Topsøe, *J. Catal.*, **187**, 109 (1999).
23. P. Raybaud, J. Hafner, G. Kresse, S. Kasztelan and H. Toulhoat, *J. Catal.*, **189**, 129 (2000).
24. H. Ge, X. Li, Z. Qin, Z. Lü and J. Wang, *Catal. Commun.*, **9**, 2578 (2008).
25. H. Ge, X. Li, W. Fan, Z. Qin, Z. Lü and J. Wang, *Chin. J. Catal.*, **30**, 111 (2009).
26. N. Rueda, R. Bacaud and M. Vrinat, *J. Catal.*, **169**, 404 (1997).
27. H. Topsøe, B. Hinnemann, J. K. Nørskov, J. V. Lauritsen, F. Besenbacher, P. L. Hansen, G. Hytoft, R. G. Egeberg and K. G. Knudsen, *Catal. Today*, **12**, 107 (2005).
28. G. Plazenet, E. Payen, J. Lynch and B. Rebours, *J. Phys. Chem. B*, **106**, 7013 (2002).
29. R. Berhault, A. Mehta, A. C. Pavel, J. Z. Yang, L. Rendon, M. J. Yácaman, L. C. Araiza, A. D. Moller and R. R. Chianelli, *J. Catal.*, **198**, 9 (2001).
30. S. Texier, G. Berhault, G. Pérot and F. Diehl, *Appl. Catal. A*, **293**, 105 (2005).
31. V. La Parola, G. Deganello and A. M. Venezia, *Appl. Catal. A*, **260**, 237 (2004).
32. H. Y. Shang, C. G. Liu, R. Y. Zhao, M. B. Wu and F. Wei, *Chin. J. Chem.*, **22**, 1250 (2004).
33. J. F. Paul, S. Cristol and E. Payen, *Catal. Today*, **130**, 139 (2008).
34. D. Ferdous, A. K. Dalai and J. Adjaye, *Appl. Catal. A*, **260**, 137 (2004).
35. N. Y. Topsøe and H. Topsøe, *J. Catal.*, **139**, 631 (1993).
36. S. Blashka, G. Bond and D. Ward, *Oil Gas J.*, **96**, 36 (1998).
37. H. Ge, X. Li, J. Wang, Z. Lü, Z. Qin and L. Zhou, *J. Fuel Chem. Technol.*, **37**, 199 (2009).
38. B. Scheffer, P. Arnoldy and J. A. Moulijn, *J. Catal.*, **112**, 516 (1988).
39. B. Scheffer, E. M. van Oers, P. Arnoldy, V. J. H. de Beer and J. A. Moulijn, *Appl. Catal.*, **25**, 303 (1986).
40. A. M. de Jong, H. J. Borg, L. J. van Ijzendoorn, V. G. F. M. Soudant, V. H. J. de Beer, J. A. R. van Veen and J. W. Niemantsverdriet, *J. Phys. Chem.*, **97**, 6477 (1993).
41. J. C. Muijsers, T. H. Weber, R. M. van Hardeveld, H. W. Zandbergen and J. W. Niemantsverdriet, *J. Catal.*, **157**, 698 (1995).
42. B. Guichard, M. Roy-Augerger, E. Devers, C. Legens and P. Ray-

- baud, *Catal. Today*, **130**, 97 (2008).
43. R. Candia, O. Sørensen, J. Villadsen, N. Y. Topsøe, B. S. Clausen and H. Topsøe, *Bull. Soc. Chim. Belg.*, **93**, 763 (1984).
44. H. Topsøe and B. S. Clausen, *Appl. Catal.*, **25**, 273 (1986).
45. M. Sun, D. Nicosia and R. Prins, *Catal. Today*, **86**, 173 (2003).
46. L. Medici and R. Prins, *J. Catal.*, **163**, 28 (1996).
47. T. Fujikawa, H. Kimura, K. Kiriya and K. Hagiwara, *Catal. Today*, **111**, 188 (2006).
48. T. F. Hayden, J. A. Dumesic, R. D. Sherwood and R. T. K. Baker, *J. Catal.*, **105**, 299 (1987).
49. J. P. R. Vissers, B. Scheffer, J. H. J. de Beer, J. A. Moulijn and R. Prins, *J. Catal.*, **105**, 277 (1987).
50. J. A. R. van Veen, E. Gerkema, A. M. van der Kraan and A. Knoester, *Chem. Commun.*, 1684 (1987).
51. S. P. A. Louwers, M. W. J. Crajé, A. M. van der Kraan, C. Geantet and R. Prins, *J. Catal.*, **144**, 579 (1993).
52. V. M. Browne, S. P. A. Louwers and R. Prins, *Catal. Today*, **10**, 345 (1991).
53. Usman, T. Yamamoto, T. Kubota and Y. Okamoto, *Appl. Catal.*, **328**, 219 (2007).
54. S. Yamada, W. Qian, A. Ishihara, G. Wang, L. Li and T. Kabe, *Sekiyu Gakkaishi*, **44**, 217 (2001).
55. C. L. Chen, C. H. Wang and H. S. Weng, *Chemosphere*, **56**, 425 (2004).